Eur. Phys. J. C (2015) 75:142
DOI 10.1140/epjc/s10052-015-3370-4

THE EUROPEAN PHYSICAL JOURNAL C

Regular Article - Theoretical Physics

Scalar clouds in charged stringy black hole-mirror system

Ran Li[a], **Junkun Zhao, Xinghua Wu, Yanming Zhang**

Department of Physics, Henan Normal University, Xinxiang 453007, China

Received: 30 January 2015 / Accepted: 20 March 2015 / Published online: 9 April 2015

Abstract It was reported that massive scalar fields can form bound states around Kerr black holes (Herdeiro and Radu, Phys. Rev. Lett. 112:221101, 2014). These bound states are called scalar clouds; they have a real frequency $\omega = m\Omega_{\rm H}$, where m is the azimuthal index and $\Omega_{\rm H}$ is the horizon angular velocity of Kerr black hole. In this paper, we study scalar clouds in a spherically symmetric background, i.e. charged stringy black holes, with the mirror-like boundary condition. These bound states satisfy the superradiant critical frequency condition $\omega = q\Phi_{\rm H}$ for a charged scalar field, where q is the charge of the scalar field, and $\Phi_{\rm H}$ is the horizon's electrostatic potential. We show that, for the specific set of black hole and scalar field parameters, the clouds are only possible for specific mirror locations $r_{\rm m}$. It is shown that analytical results of the mirror location $r_{\rm m}$ for the clouds perfectly coincide with numerical results in the $qQ \ll 1$ regime. We also show that the scalar clouds are also possible when the mirror locations are close to the horizon. Finally, we provide an analytical calculation of the specific mirror locations $r_{\rm m}$ for the scalar clouds in the $qQ \gg 1$ regime.

1 Introduction

It was firstly proposed by Hod that a scalar field can have real bound states in the near-extremal Kerr black hole [1,2]. Soon later, it was reported in [3] that massive scalar fields can form bound states around Kerr black holes by using the numerical method to solve the scalar field equation in the background. These bound states are the stationary scalar configurations in the black hole backgrounds, which are regular at the horizon and outside. They are named scalar clouds. More importantly, it was shown that the backreaction of clouds can generate a new family of Kerr black holes with scalar hair [3,4]. It is suggested that whenever clouds of a given matter field can be found around a black hole, in a linear analysis, there exists a fully non-linear solution of a new hairy black hole correspondingly. However, it requires that the field generating the clouds yields a time independent energy-momentum tensor. Generally, the field should be complex and have a factor $e^{-i\omega_c t}$, where ω_c is the superradiance critical frequency. For instance, real scalar fields can give rise to clouds but not hairy black holes [5]. So, it seems that the studies of scalar clouds at the linear level are very important for us to find hairy black holes at the non-linear level. This subject has attracted a lot of attention recently [6–16].

Generally speaking, the existence of stationary bound states of matter fields in black hole backgrounds requires two necessary conditions. The first is that the matter fields should undergo the classical superradiant phenomenon [17,18] in the black hole background. This condition can be satisfied by the bosonic fields in the rotating black holes or the charged scalar fields in the charged black holes [19]. When the frequencies of these matter fields ω are smaller than the superradiant critical frequency ω_c, there are time growing quasi-bound states. When $\omega > \omega_c$, the fields are time decaying. So, the scalar clouds exist at the boundary between these two regimes, i.e. the frequencies of the fields are taken as the superradiant critical frequency ω_c. For the rotating black holes, the critical frequency ω_c is $m\Omega_{\rm H}$, where m is the azimuthal index and $\Omega_{\rm H}$ is the horizon angular velocity. For the charged black holes, $\omega = q\Phi_{\rm H}$, where q is the charge of the scalar field, and $\Phi_{\rm H}$ is the horizon's electrostatic potential. The second one is there should be a potential well outside the black hole horizon in which the bound states can be trapped. This potential well may be provided by the mass term of the field, i.e. $\omega < \mu$, where μ is the mass of the scalar field. However, sometimes the artificial boundary conditions can play the same role.

In this paper, we will study the scalar clouds in a spherically symmetric and charged background. Specifically, we will consider the charged scalar field in the backgrounds of charged stringy black holes. At first sight, it seems that the massive scalar field can form the clouds in this background.

[a] e-mail: 021149@htu.cn

However, it is proved that the massive charged scalar field is stable in this background and there is no superradiant instability [20]. To generate the superradiant instability [21,22], the mirror-like boundary condition should be imposed according to the black hole bomb mechanism [23,24]. Analytical and numerical studies of this subject can be found in [25] and [26]. Correspondingly, the scalar clouds are only possible with the mirror-like boundary condition. Using numerical methods, we will study the dynamics of the massless charged scalar field satisfying the frequency condition $\omega = q\Phi_{\rm H}$ and the mirror-like boundary condition. We will show that, for the specific set of black hole and scalar field parameters, the clouds are only possible for the specific mirror locations $r_{\rm m}$. It will be shown that the analytical results of the mirror location $r_{\rm m}$ for the clouds perfectly coincide with the numerical results. In addition, we will show that the scalar clouds are also possible when the mirror locations are close to the horizon. Finally, we will provide an analytical calculation of the specific mirror locations $r_{\rm m}$ for the scalar clouds in the $qQ \gg 1$ regime.

This paper is organized as follows. In Sect. 2, we will present the background geometry of a charged string black hole and the dynamic equation of the scalar field. In particularly, we will give the superradiant condition and the boundary condition of this black hole–mirror system. In Sect. 3, we describe the numerical procedure to solve the radial equation under a certain boundary condition. In this section, the numerical results are illustrated. Some general discussions of the numerical results are also presented. In Sect. 4, an analytical calculation of the mirror radius $r_{\rm m}$ for scalar clouds in the $qQ \gg 1$ regime is presented. The conclusion is in Sect. 5.

2 Description of the system

We shall consider a massless charged scalar field minimally coupled to the charged stringy black hole with the mirror-like boundary condition. The black hole is a static spherically symmetric charged black hole in the low energy effective theory of heterotic string theory in four dimensions, which was first found by Gibbons and Maeda in [27] and independently found by Garfinkle et al. in [28] a few years later. The metric is given by

$$\begin{aligned} {\rm d}s^2 =& -\left(1-\frac{2M}{r}\right){\rm d}t^2+\left(1-\frac{2M}{r}\right)^{-1}{\rm d}r^2 \\ &+r\left(r-\frac{Q^2}{M}\right)({\rm d}\theta^2+\sin^2\theta{\rm d}\phi^2), \end{aligned} \tag{1}$$

and the electric potential and the dilaton field

$$A_{\rm t} = -\frac{Q}{r}, \tag{2}$$

$$e^{2\Phi} = 1-\frac{Q^2}{Mr}. \tag{3}$$

The parameters M and Q are the mass and the electric charge of the charged stringy black hole, respectively. The event horizon of the black hole is located at $r = 2M$. The area of the sphere approaches zero when $r = Q^2/M$. Therefore, the sphere surface of the radius $r = Q^2/M$ is singular. When $Q^2 \le 2M^2$, this singular surface is surrounded by an event horizon. In this paper, we will always assume the cosmic censorship hypothesis, i.e. we will only consider black holes with the parameters satisfying the condition $Q^2 \le 2M^2$.

The dynamics of the charged scalar field is then governed by the Klein–Gordon equation

$$(\nabla_\nu - iqA_\nu)(\nabla^\nu - iqA^\nu)\Psi = 0, \tag{4}$$

where q denotes the charge of the scalar field. By taking the ansatz of the scalar field $\Psi = e^{-i\omega t}R(r)Y_{lm}(\theta,\phi)$, where ω is the conserved energy of the mode, l is the spherical harmonic index, and m is the azimuthal harmonic index with $-l \le m \le l$, one can deduce the radial wave equation in the form of

$$\Delta\frac{\rm d}{{\rm d}r}\left(\Delta\frac{{\rm d}R}{{\rm d}r}\right)+UR = 0, \tag{5}$$

where we have introduced a new function $\Delta = (r-r_+)(r-r_-)$ with $r_+ = 2M$ and $r_- = Q^2/M$, and the potential function is given by

$$U = \left(r-\frac{Q^2}{M}\right)^2(\omega r - qQ)^2 - \Delta l(l+1). \tag{6}$$

The superradiant condition of the charged scalar field is given by

$$\omega < q\Phi_{\rm H}, \tag{7}$$

where $\Phi_{\rm H} = \frac{Q}{2M}$ is the electric potential at the horizon [20,29,30]. It is proved in [20] that the massive charged scalar field is stable in this black hole background. To have superradiant instability, we should impose the mirror-like boundary condition [25,26]. In order to study the bound states, we shall focus on the critical case that the scalar frequency equals the superradiant critical frequency, i.e.

$$\omega = q\Phi_{\rm H}. \tag{8}$$

To solve the radial equation (5), we should impose the following boundary conditions:

$$R(r) = \begin{cases} R_0(1+\sum_{k\ge1}R_k(r-r_+)^k), & r\to r_+, \\ 0, & r = r_{\rm m}. \end{cases} \tag{9}$$

The first line indicates that the scalar field is regular near the horizon and the second line implies that the system is placed in a perfectly reflecting cavity.

3 Numerical procedure and results

The numerical methods employed in this problem are based on the shooting method, which is also called the direct integration (DI) method [31–34]. It is shown that the DI method is specially suited to find a stationary field configuration with the mirror-like boundary condition.

Firstly, near the event horizon $r = 2M$, we require that the radial function is regular and expand the radial function $R(r)$ as a generalized power series in terms of $(r - r_+)$ as in the first line of Eq. (9). Because the radial equation is linear, we can take $R_0 = 1$ without loss of generality. Substituting the expansion of the radial wave function into the radial equation (5), we can solve the coefficient R_k order by order in terms of $(r - r_+)$. We have only considered six terms in the expansion. The R_ks can be expressed in terms of the parameters (M, Q, q, l), which are not exhibited here.

Then we can integrate the radial equation (5) from $r = r_+(1 + \epsilon)$ and stop the integration at the radius of the mirror. In this procedure, we have taken the small ϵ as 10^{-6}. The procedure can be repeated by varying the input parameters (M, Q, q, l) until the mirror-like boundary condition $R(r_{\rm m}) = 0$ is reached with the desired precision. We can use a numerical root finder to search the location of the mirror that supports the stationary scalar configuration. We have found that, for the given input parameters (M, Q, q, l), scalar clouds exist for a discrete set of $r_{\rm m}$, which is labeled by the quantum number n of nodes of the radial function $R(r)$.

Firstly, we make a comparison of the numerical and analytical results. From the analytical result Eq. (35) in Ref. [25], one can obtain the mirror radius that supports the scalar cloud; it can be approximately given by

$$r_{\rm m} = \frac{j_{l+1/2,n'}}{q\Phi_{\rm H}}. \tag{10}$$

We have labeled the n'th positive zero of the Bessel function $J_{l+1/2}$ as $j_{l+1/2,n'}$. The numerical results show that this "quantum number" is closely connected with the node number n of the radial function $R(r)$ considering the simple relation $n = n' - 1$. It should be noted that this analytical expression for the mirror radius is only valid for the case of $qQ \ll 1$. With the condition $qQ \ll 1$, the asymptotic expansion matching method can be employed to solve the radial equation approximately [25]. In Fig. 1, we have displayed the analytical results and the numerical results of the mirror location $r_{\rm m}$ in terms of the black hole charge Q. Here, we do not consider the naked singularity spacetime, so that the value range of the black hole charge Q is $(0, \sqrt{2}]$, where we have fixed the black hole mass as $M = 1$. It is shown that the analytical results of the mirror location $r_{\rm m}$ for the clouds perfectly coincide with the numerical results, even in the region where the analytical approximation is non-applicable. When $q = 0.2$, the analytical approximation is always precise in the whole range of Q. When $q = 0.8$, the analytical results show an obvious difference with the numerical results only for large Q.

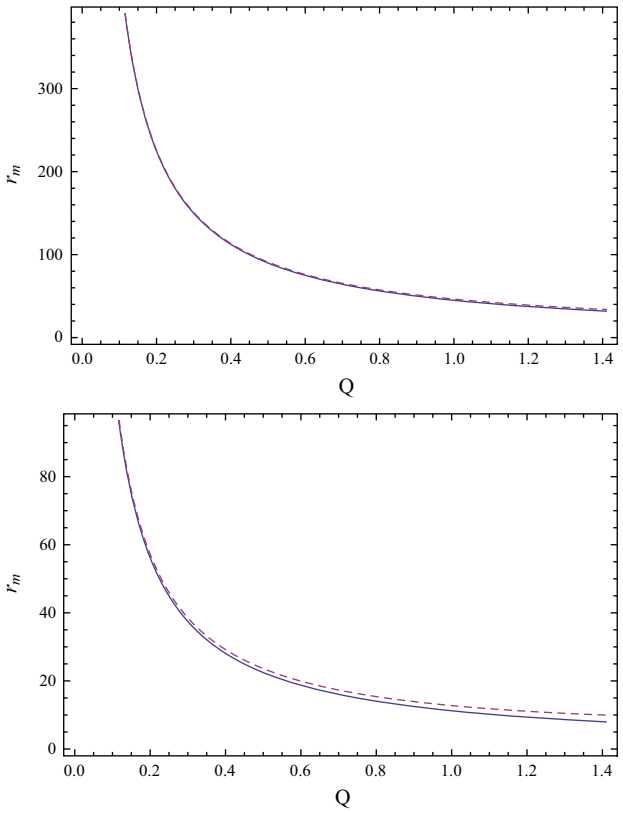

Fig. 1 Mirror location $r_{\rm m}$ plotted versus the black hole charge Q for $M = 1, l = 1, n = 0$ and for various scalar charges q. For the *first panel*, $q = 0.2$, while for the *second panel*, $q = 0.8$. The *solid line* and the *dashed line* represent the analytical and the numerical results, respectively

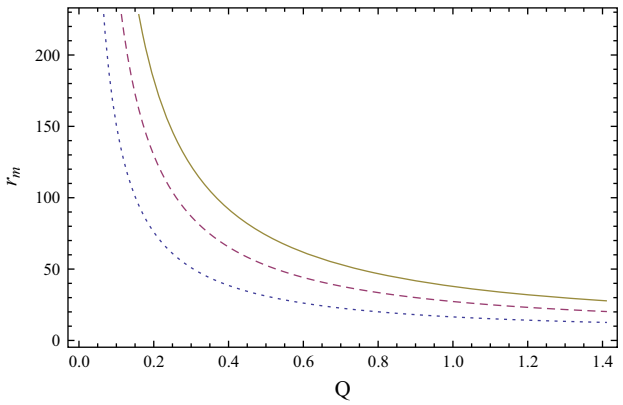

Fig. 2 Mirror location $r_{\rm m}$ plotted versus the black hole charge Q for $M = 1, l = 1, q = 0.6$ and for various node numbers n. The *dotted*, *dashed*, and *solid lines* represent $n = 0$, 1, and 2, respectively

In Fig. 2, we have drawn the mirror location $r_{\rm m}$ that supports the scalar cloud as a function of the black hole charge Q for various values of the node number n of the radial function.

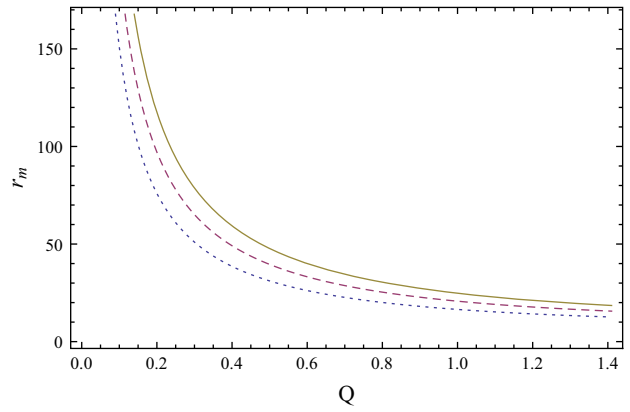

Fig. 3 Mirror location $r_{\rm m}$ plotted versus the black hole charge Q for $M = 1, n = 0, q = 0.6$, and for various l. The *dotted*, *dashed*, and *solid lines* represent $l = 1, 2$, and 3, respectively

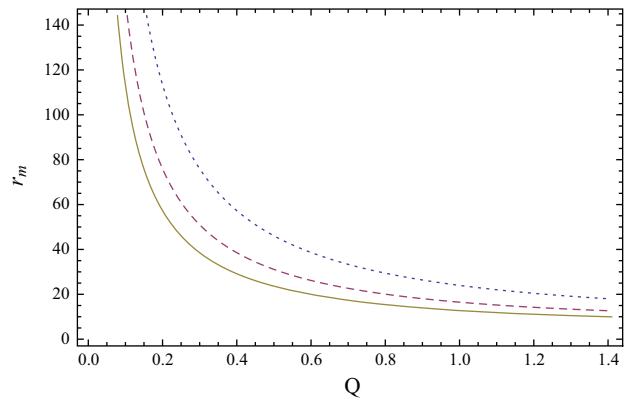

Fig. 4 Mirror location $r_{\rm m}$ plotted versus the black hole charge Q for $M = 1, l = 1, n = 0$ and for various scalar charges q. The *dotted*, *dashed*, and *solid lines* represent $q = 0.4, 0.6$, and 0.8, respectively

It is observed that when the black hole charge Q increases, we need to place the reflecting mirror closer to the horizon in order to have a scalar cloud. When the node number n of the radial function increases, the plotted lines go away from the axis. This observation coincides with the analytical result (10) in the regime of $qQ \ll 1$.

In Figs. 3 and 4, we display the mirror location $r_{\rm m}$ as a function of the black hole charge Q for various l and q. We can observe that the lines go far away from the axis when increasing l, while the lines go closer to the axis when increasing the scalar charge q. This is also expected from the analytical result (10). In addition, Figs. 3 and 4 together with Fig. 2 show that, when $Q \to 0$, $r_{\rm m} \to \infty$. This indicates that there is no massless scalar cloud for the Schwarzschild black hole with the mirror-like boundary condition [16], even though it is possible for massive scalar fields in a Schwarzschild black hole to have arbitrarily long-lived quasi-bound states [35].

We also consider the radial dependence of the massless scalar clouds. In Figs. 5 and 6, we have fixed the mirror radius as $r_{\rm m} = 40$. We can solve the radial equation numerically

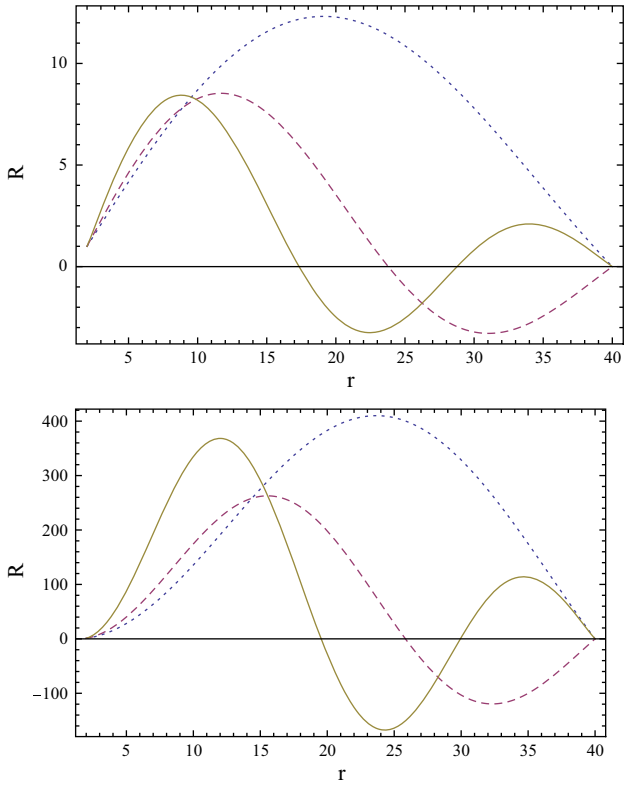

Fig. 5 Radial functions $R(r)$ of scalar clouds for $M = 1, q = 0.6, r_{\rm m} = 40$ with different harmonic indices l and node numbers n. The *first* and the *second panels* correspond to $l = 1$ and 2, respectively. The *dotted*, *dashed*, and *solid lines* represent $n = 1, 2$, and 3, respectively

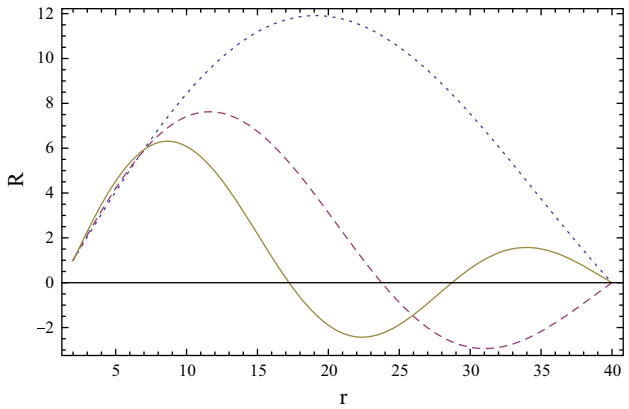

Fig. 6 Radial functions $R(r)$ of scalar clouds for $M = 1, q = 0.8, l = 1, r_{\rm m} = 40$ with different node number n. The *dotted*, *dashed*, and *solid lines* represent $n = 1, 2$, and 3, respectively, and the corresponding black hole charge Q are 0.219882, 0.583819, and 0.956562

and obtain a discrete set of black hole charges Q, labeled by the node number n of the radial wave equation. Then we can integrate the radial equation for the fixed node numbers and obtain the corresponding numerical solutions of the radial wave functions. It is shown that the radial profile has the typical forms of standing waves with the fixed boundary

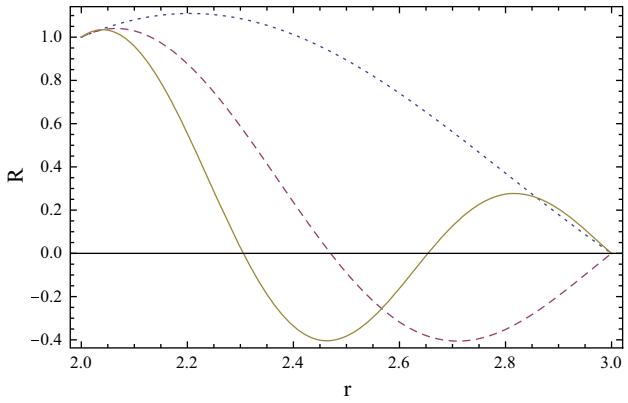

Fig. 7 Radial functions $R(r)$ of scalar clouds for the small mirror radius $r_{\rm m} = 3$. The parameters of the black hole and the scalar field are taken as $M = 1$, $q = 20$, and $l = 1$. The *dotted*, *dashed*, and *solid lines* represent $n = 1, 2$, and 3, respectively, and the corresponding black hole charges Q are 0.306384, 0.600699, 0.913741

conditions. We have also calculated the case that $l = 3$. The results are not presented here. The general form of the radial wave function is similar to the profiles in Fig. 5.

In Fig. 7, we consider the case that the mirror location is very close to the horizon. We take the mirror radius as $r_{\rm m} = 3$. From our previous analytical and numerical work on the superradiant instability of the scalar field in the background of the charged stringy black hole plus mirror system, we need a large scalar field charge q. Here, we set $q = 20$. We can see that the scalar field can be bounded by the reflecting mirror very close to the horizon to form the clouds. The radial wave functions in this case have similar profiles to Figs. 5 and 6.

4 Scalar clouds in $qQ \gg 1$ regime

In the above numerical calculations, we find that the radial equation becomes hard to integrate when the scalar charge q is large. So it is important to make an analytical study of the stationary charged scalar clouds in the $qQ \gg 1$ regime. In this section, we will give an analytical expression of the special mirror radius $r_{\rm m}$ in the $qQ \gg 1$ limit, for which the charged scalar field can be confined to form a stationary cloud configuration.

Following [36], it is convenient to introduce the new dimensionless variables

$$x = \frac{r - r_+}{r_+}, \quad \tau = \frac{r_+ - r_-}{r_+}, \tag{11}$$

in terms of which the radial equation (5) becomes

$$x(x+\tau)\frac{{\rm d}^2R}{{\rm d}x^2} + (2x+\tau)\frac{{\rm d}R}{{\rm d}x} + [q^2Q^2x(x+\tau) - l(l+1)]R = 0, \tag{12}$$

where we have set the superradiance critical frequency $\omega = q\Phi_{\rm H}$ in the above equation.

This equation can be solved by a Bessel function in the double limit

$$qQ \gg 1, \quad x \ll \tau. \tag{13}$$

In this asymptotic regime, the radial equation can be reduced to

$$x\frac{{\rm d}^2R}{{\rm d}x^2} + \frac{{\rm d}R}{{\rm d}x} + q^2Q^2xR = 0. \tag{14}$$

The solution is then given by the Bessel function of the first kind

$$R(x) = J_0(qQx), \tag{15}$$

i.e., the stationary scalar field is then described by the above function. By taking account of the mirror-like boundary condition $R(x_{\rm m}) = 0$, we can obtain the special mirror radius $r_{\rm m}$ as

$$r_{\rm m} = 2M + \frac{j_{0,n}}{q\Phi_{\rm H}}, \quad n = 1, 2, 3, \ldots \tag{16}$$

where $j_{0,n}$ is the nth positive zero of the Bessel function $J_0(x)$. From this expression, we can see that, when $qQ \gg 1$, the reflecting mirror should be placed very close to the horizon to form the cloud configuration. This is consistent with the near horizon condition $x \ll \tau$.

5 Conclusion

In summary, in this paper, we have studied the massless scalar clouds in the charged stringy black holes with the mirror-like boundary conditions. The scalar clouds are stationary bound states satisfying the superradiant critical frequency $\omega = q\Phi_{\rm H}$. The scalar clouds in rotating black holes [3,8] can be heuristically interpreted in terms of a mechanical equilibrium between the black hole-cloud gravitational attraction and angular momentum driven repulsion. For the charged black hole cases, the charged clouds cannot be formed, because gravitational attraction and electromagnetic repulsion cannot reach equilibrium [7]. An additional mirror should be placed at a special location to reflect the charged scalar wave.

We show that, for the specific set of black hole and scalar field parameters, the clouds are only possible for the specific mirror location $r_{\rm m}$. For example, for the fixed parameters of black hole and scalar field M, Q, q, l, the discrete set of the mirror location $r_{\rm m}$ is characterized by the node number n of the radial wave function. It is shown that the analytical results of the mirror location $r_{\rm m}$ for the clouds perfectly coincide with the numerical results in the region

of $qQ \ll 1$. However, the agreement becomes less impressive for $qQ = O(1)$ values. In addition, we also show that the massless scalar clouds are also possible when the mirror locations are very close to the horizon. Finally, we present an analytical calculation of the specific mirror locations $r_{\rm m}$ for the scalar clouds in the $qQ \gg 1$ regime.

Acknowledgments The authors would like to thank Dr. Hongbao Zhang for useful discussion on the numerical methods. This work was supported by NSFC, China (Grant No. 11205048).

References

1. S. Hod, Phys. Rev. D **80**, 104026 (2012)
2. S. Hod, Eur. Phys. J. C **73**, 2378 (2013)
3. C.A.R. Herdeiro, E. Radu, Phys. Rev. Lett. **112**, 221101 (2014)
4. C.A.R. Herdeiro, E. Radu, Phys. Rev. D **89**, 124018 (2014)
5. C. Herdeiro, E. Radu, arXiv:1501.04319 [gr-qr]
6. S. Hod, Phys. Rev. D **90**, 024051 (2014)
7. J. Degollado, C. Herdeiro, Gen. Rel. Grav. **45**, 2483 (2013)
8. C. Benone, L. Crispino, C. Herdeiro, E. Radu, Phys. Rev. D **90**, 104024 (2014)
9. M. Sampaio, C. Herdeiro, M. Wang, Phys. Rev. D **90**, 064004 (2014)
10. A. Graham, R. Jha, Phys. Rev. D **90**, 041501 (2014)
11. J. Degollado, C. Herdeiro, Phys. Rev. D **90**, 065019 (2014)
12. Y. Brihaye, C. Herdeiro, E. Radu, Phys. Lett. B **739**, 1 (2014)
13. C. Herdeiro, E. Radu, H. Runarsson, Phys. Lett. B **739**, 302 (2014)
14. S. Hod, Phys. Lett. B **739**, 196 (2014)
15. S. Hod, Phys. Lett. B **736**, 398 (2014)
16. C. Benone, L. Crispino, C. Herdeiro, E. Radu, arXiv:1412.7278 [gr-qc]
17. J.M. Bardeen, W.H. Press, S.A. Teukolsky, Astrophys. J. **178**, 347 (1972)
18. C.W. Misner, Bull. Am. Phys. Soc. **17**, 472 (1972)
19. J.D. Bekenstein, Phys. Rev. D **7**, 949 (1973)
20. R. Li, Phys. Rev. D **88**, 127901 (2013)
21. S. Detweiler, Phys. Rev. D **22**, 2323 (1980)
22. H. Furuhashi, Y. Nambu. Prog. Theor. Phys. **112**, 983 (2004)
23. W.H. Press, S.A. Teukolsky, Nature (London) **238**, 211 (1972)
24. V. Cardoso, O.J.C. Dias, J.P.S. Lemos, S. Yoshida, Phys. Rev. D **70**, 044039 (2004)
25. R. Li, J. Zhao, Eur. Phys. J. C **74**, 3051 (2014)
26. R. Li, J. Zhao, Phys. Lett. B **740**, 317 (2015)
27. G.W. Gibbons, K. Maeda, Nucl. Phys. B **298**, 741 (1998)
28. D. Garfinkle, G.T. Horowitz, A. Strominger, Phys. Rev. D **43**, 3140 (1991)
29. K. Shiraishi, Mod. Phys. Lett. A **7**, 3449 (1992)
30. J. Koga, K. Maeda, Phys. Lett. B **340**, 29 (1994)
31. J.C. Degollado, C.A.R. Herdeiro, H.F. Runarsson, Phys. Rev. D **88**, 063003 (2013)
32. S.R. Dolan, L.A. Oliveira, L.C.B. Crispino, Phys. Rev. D **82**, 084037 (2010)
33. L.A. Oliveira, V. Cardoso, L.C.B. Crispino, Phys. Rev. D **89**, 124008 (2014)
34. N. Uchikata, S. Yoshida, T. Futamase, Phys. Rev. D **80**, 084020 (2009)
35. J. Barranco et al., Phys. Rev. Lett. **109**, 081102 (2012)
36. S. Hod, Phys. Rev. D **88**, 064055 (2013)